

## Gamma-Ray Decay Schemes for $^{89}\text{Kr}$ and $^{89}\text{Rb}$

E. A. Henry, W. L. Talbert, Jr., and J. R. McConnell

Ames Laboratory, USAEC and Department of Physics, Iowa State University, Ames, Iowa 50010

(Received 21 August 1972)

A study has been made of  $\gamma$ -ray deexcitations following the  $\beta$  decays of  $^{89}\text{Kr}$  and  $^{89}\text{Rb}$ . The activities were produced from the TRISTAN on-line isotope-separator system. Measurements of  $\gamma$ -ray energies and intensities were made using Ge(Li) detectors. Level schemes have been constructed for  $^{89}\text{Rb}$  and  $^{89}\text{Sr}$  with the aid of  $\gamma$ - $\gamma$  coincidence information, and  $\beta$  branching was determined from equilibrium data and  $\gamma$ -intensity balances. The excited levels of  $^{89}\text{Sr}$  appear to be explained by single-particle states and the coupling of single-particle states to the vibration states of  $^{88}\text{Sr}$ . The  $^{89}\text{Rb}$  nucleus is shown to have a complex level scheme and will require further studies to clarify the picture of its nuclear structure.

### I. INTRODUCTION

This study of  $\gamma$ -ray deexcitation following the  $\beta$  decays of  $^{89}\text{Kr}$  and  $^{89}\text{Rb}$  is part of a systematic study of the decays of short-lived gaseous fission products<sup>1-5</sup> undertaken at the TRISTAN on-line isotope-separator facility.<sup>6</sup> Because of its nearness to  $^{88}\text{Sr}$  and  $^{90}\text{Zr}$ , the  $^{89}\text{Sr}$  nucleus has been the subject of many studies including  $\gamma$ -ray spectroscopy,<sup>7</sup> stripping reaction,<sup>8-10</sup> and isobaric-analog studies.<sup>11-13</sup> The wealth of experimental information available and the comparative simplicity of the  $^{89}\text{Sr}$  nucleus have made it the subject of theoretical studies as well.<sup>14-16</sup> On the other hand, the  $^{89}\text{Rb}$  nucleus is more difficult to study experimentally than is the  $^{89}\text{Sr}$  nucleus, and to date only  $\gamma$ -ray spectroscopy of the decay of  $^{89}\text{Kr}$  has been performed.<sup>17,18</sup>

Comprehensive studies reported by Kitching and Johns<sup>7,17</sup> at McMaster University on the decays of  $^{89}\text{Rb}$  (1966) and  $^{89}\text{Kr}$  (1967) used state-of-the-art Ge(Li) detectors and electronics, and chemically separated sources. They observed about 15  $\gamma$  rays from the decay of  $^{89}\text{Rb}$  and established a level scheme for  $^{89}\text{Sr}$  with eight excited levels with the aid of  $\gamma$ - $\gamma$  and  $\beta$ - $\gamma$  coincidence information. Using a magnetic spectrometer, a value of  $4.486 \pm 0.012$  MeV was obtained for  $Q_\beta$  for the  $^{89}\text{Rb}$  decay.

For the decay of  $^{89}\text{Kr}$ , Kitching and Johns reported a very complex  $\gamma$ -ray spectrum with more than 130 peaks. With the aid of  $\gamma$ - $\gamma$  and  $\beta$ - $\gamma$  coincidence information, the  $\gamma$  rays were placed in a proposed level scheme for  $^{89}\text{Rb}$  with 33 excited levels. Using the  $\beta$ - $\gamma$  coincidence information, a  $Q_\beta$  value of  $5.15 \pm 0.03$  MeV was obtained for the  $^{89}\text{Kr}$  decay with about 0.1%  $\beta$  feeding to the ground state of  $^{89}\text{Rb}$ . In recent work (1972) at the same laboratory, Poehlman<sup>18</sup> observed about 170 photo-peaks in the decay of  $^{89}\text{Kr}$  and placed 123 of them in a level scheme for  $^{89}\text{Rb}$  with 34 excited levels. In the present work, use of mass-separated

sources revealed some meaningful transitions which were masked by other krypton and rubidium contaminants from the chemically obtained sources of Kitching and Johns and of Poehlman.

The  $^{88}\text{Sr}(d, p)^{89}\text{Sr}$  stripping reaction was used by Preston, Sampson, and Marten<sup>9</sup> to establish experimentally the similarity between the  $^{89}\text{Sr}$  and  $^{91}\text{Zr}$  nuclei. The single-particle levels in  $^{89}\text{Sr}$  populated by the neutron outside the  $N=50$  closed shell, as well as some particle-core coupled levels, were identified by Cosman, Enge, and Sperduto<sup>10</sup> using stripping reactions. The study of the isobaric-analog states of  $^{89}\text{Sr}$  by use of the  $^{88}\text{Sr}(p, p)$  and  $^{88}\text{Sr}(p, p')$  reactions by Cosman *et al.*<sup>11-13</sup> has extended the interpretation of the  $^{89}\text{Sr}$  excited levels in terms of the particle-core model.

In the present work,  $\gamma$ -ray transition energies and relative intensities are reported for the  $^{89}\text{Kr}$  and  $^{89}\text{Rb}$  decays and, with the aid of  $\gamma$ - $\gamma$  coincidence information, level schemes are constructed for the  $^{89}\text{Sr}$  and  $^{89}\text{Rb}$  nuclei. The percent  $\beta$  branching to each level and the associated  $\log ft$  values are deduced from the level schemes. Tentative spin and parity assignments for the levels of  $^{89}\text{Sr}$  and  $^{89}\text{Rb}$  are based mainly on  $\log ft$  values, relative  $\gamma$ -ray transition probabilities, and nuclear systematics near mass 89. The previously mentioned reaction work is useful in removing ambiguous spin and parity assignments in the case of  $^{89}\text{Sr}$ . The single-particle and particle-core coupled level configurations proposed for  $^{89}\text{Sr}$  are suggested by the spin and parity assignments in the present work, the  $\gamma$  transitions seen between levels, surveys of neighboring nuclei, and comparison of the present results with those of reaction studies.

### II. PROCEDURE

#### A. Experimental Arrangement

Samples of  $^{89}\text{Kr}$  are obtained from the thermal-neutron-induced fission of  $^{235}\text{U}$  using the TRISTAN

facility. The uranium, in the form of uranium stearate, is placed in an evacuated container and exposed to an external neutron beam with a flux of  $3 \times 10^9 n_{\text{th}}/\text{cm}^2 \text{sec}$  at the Ames Laboratory research reactor. The gaseous fission products are introduced through a transport line to the ion source of an electromagnetic isotope separator which makes possible the isotopic selection. The  $^{89}\text{Kr}^+$  ion beam is selected at the focal plane of the separator and guided by a switch magnet to the moving tape collector where radiation detectors are placed. The only contaminants observed while collecting  $^{89}\text{Kr}$  in this experiment were due to mass 88 activities, resulting from a small amount of  $^{88}\text{KrH}^+$  ions in the ion beam, and certain background activities.

The capabilities of the moving tape collector<sup>19</sup> were exploited to provide isobaric separation of the parent and daughter activities. Two 58-cm<sup>3</sup> Ge(Li) true coaxial detectors were used to observe each decay, with  $\gamma$ -ray singles data taken using 8192-channel resolution. Constant-fraction timing circuitry was used in coincidence data accumulation with all observed coincidence events being recorded in a 4096 $\times$ 4096 format on a buffered tape system. A 1-cm<sup>3</sup> planar low-energy photon spectrometer was used to observe  $\gamma$  rays with energies between 10 and 197 keV.

#### B. Data Accumulation and Analysis

For each singles-data accumulation, four spectra were obtained: a background spectrum, a calibration-source spectrum, an unknown-plus-calibration-source spectrum, and an unknown spectrum. The unknown spectrum usually consisted of either primarily parent or primarily daughter activity, as a result of using the moving tape collector.

The moving tape collector, when operated in a continuous transport mode, allowed strong enhancement of the  $^{89}\text{Kr}$  parent activity ( $T_{1/2} = 3.2$  min) by continuous removal from the source position of the  $^{89}\text{Rb}$  daughter activity ( $T_{1/2} = 15.4$  min). In this parent-enhanced run, the integrated activity observed was 99.8%  $^{89}\text{Kr}$ , 0.2%  $^{89}\text{Rb}$ , and negligible  $^{89}\text{Sr}$ , according to calculations using the program ISOBAR.<sup>19</sup> The daughter activity was enhanced by using a discontinuous transport mode with a delay time before the start of data accumulation to allow the parent to decay away. Using the discontinuous mode of operation, the integrated activity observed was 92.1%  $^{89}\text{Rb}$ , 7.6%  $^{89}\text{Kr}$ , and 0.3% Sr, again according to ISOBAR.

In addition to the two types of enhanced runs, an equilibrium singles accumulation was taken. The separated  $^{89}\text{Kr}$  ions were deposited at a single

spot on the transport tape, and the parent and daughter activities were allowed to build to equilibrium before data accumulation started. Continuous deposition of  $^{89}\text{Kr}$  ions enabled the  $^{89}\text{Kr}$  and  $^{89}\text{Rb}$  activities to remain at equilibrium throughout the accumulation.

Spectrum-peak centroids and areas were determined for the singles data by applying a nonlinear least-squares fit of a skewed-Gaussian-fit function to the data using the IBM 360/Model 65 computer at the Iowa State University Computation Center. Using various utility routines, the centroid and area information was transformed into transition energies and intensities.

Coincidence and coincidence-background gates were digitally selected using the buffered tape control system, and all recorded events were searched to obtain coincidence and coincidence-background gate spectra. Coincidence spectra were scanned visually, and definite and possible coincidences were recorded. Coincidences were called definite if the height of the peak in question in the coincidence gate was statistically significant when compared to the same region in the coincidence-background gate. Coincidences were called possible if some indication of peaking was seen but the definite coincidence criterion was not met, or the coincidence in question was partially masked or otherwise disturbed.

#### C. Level Schemes

The construction of level schemes for  $^{89}\text{Sr}$  and  $^{89}\text{Rb}$  began by establishing several excited levels involving the most intense  $\gamma$  rays in each spectrum. These levels were easily confirmed by coincidence information, and the energy sums involved were consistent to within 50 eV or less. For new excited levels to be established, a minimum of at least three  $\gamma$  rays were required to be involved in the population and/or depopulation of the new levels to or from established levels. This requirement was relaxed only if additional information was available to confirm the new levels. This additional information could be: (1) coincidence confirmation; (2) the absence of an intense photopeak in the total coincidence profile, indicating that the photopeak depopulates to the ground state a level fed primarily by  $\beta$  decay; (3) energy sums involving a transition and the first excited level which put the new level above  $Q_{\beta}$ , indicating that the photopeak in question is a likely ground-state transition; and (4) reaction results indicating the presence of a level.

Because of the many  $\gamma$ -ray transitions and excited levels involved in these schemes, multiple placements of  $\gamma$  rays by energy sums were some-

times possible. These multiple placements were made only when the coincidence information confirmed them. In other cases of possible multiple placement, where no coincidence information was available, preference was given to placement of the transition between well established levels.

From the completed level schemes, with most of the observed  $\gamma$ -ray intensity placed, the  $\beta$  feeding to each excited level was determined from a balance of the intensities of the  $\gamma$  ray populating and depopulating that level. The ground-state  $\beta$  branch from  $^{89}\text{Kr}$  was determined in the following way through use of the equilibrium accumulation data. Using the level scheme for  $^{89}\text{Sr}$ , and assuming the 18%  $\beta$ -feeding value to the ground state of  $^{89}\text{Sr}$  determined by Kitching and Johns,<sup>7</sup> the total depopulation of the  $^{89}\text{Rb}$  ground state by  $\beta$  decay was obtained. The equilibrium data accumulation enabled the  $^{89}\text{Kr}$  and  $^{89}\text{Rb}$   $\gamma$ -ray spectra to be normalized to each other and, knowing the  $\gamma$ -ray feeding to the  $^{89}\text{Rb}$  ground state, the percent  $\beta$  feeding from  $^{89}\text{Kr}$  to the  $^{89}\text{Rb}$  ground state was determined.

### III. DATA AND RESULTS

#### A. Assignment of Transitions to $^{89}\text{Kr}$ and $^{89}\text{Rb}$ Decays

Since the use of the moving tape collector was quite effective in separating the  $^{89}\text{Kr}$  and  $^{89}\text{Rb}$  activities, assignment of the bulk of the observed photopeaks to the proper decay was made easily. However, careful comparison of the intensities of certain photopeaks in the parent-enhanced and daughter-enhanced data indicated that these transitions occurred in both spectra at nearly the same energy. The  $\gamma$  rays were assigned to both decays with the intensities apportioned to each decay being determined through use of the known activity ratios for each data accumulation. The assignment of  $\gamma$  rays of nearly the same energy to both decays is in many cases confirmed by coincidence results.  $\gamma$  rays assigned to both decays in Tables I and III are indicated by footnote.

#### B. Decay of $^{89}\text{Rb}$

Of the 62  $\gamma$  rays assigned to the decay of  $^{89}\text{Rb}$ , 49  $\gamma$  rays are placed in the  $^{89}\text{Sr}$  level scheme which has 16 excited levels. The 49 placed  $\gamma$  rays account for 99.8% of the observed  $\gamma$ -ray intensity. A summary of the  $\gamma$  rays attributed to  $^{89}\text{Rb}$  decay is given in Table I.

The  $^{89}\text{Sr}$  level scheme is shown in Fig. 1, with the transition energy and intensity per 100  $\beta$  decays identifying each  $\gamma$  ray placed in the level scheme drawing. A solid circle at the head or tail of the  $\gamma$ -ray transition arrow indicates that

definite coincidence information is available for the placement of that transition, while an open circle indicates possible coincidence relationship. A total of 13 coincidence gates was used to determine the results shown. Detailed coincidence results are not tabulated here in the interest of brevity, but are available in Henry<sup>20</sup>.

The 18% ground-state  $\beta$  branch and the  $Q_\beta$  value of  $4.486 \pm 0.012$  MeV reported by Kitching and Johns<sup>7</sup> for the decay of  $^{89}\text{Rb}$  were used in this work for  $\log ft$  calculations. The percent  $\beta$  branch to each excited level in  $^{89}\text{Sr}$  was obtained from the level scheme. In the  $\log ft$  calculations for each  $\beta$  branch, a statistical shape was assumed for the  $\beta$ -spectrum shape and atomic screening was taken into account. No allowance for internal conversion was made, since data accumulated with the low-energy photon spectrometer revealed that x rays in the 14-keV region of  $^{89}\text{Kr}$  and  $^{89}\text{Rb}$  were of very low intensity, if present at all, indicating little internal conversion. The percent  $\beta$  feeding and associated  $\log ft$  value for each level in  $^{89}\text{Sr}$  are given in Table II.

The major excited levels of  $^{89}\text{Sr}$  (involving most of the intensity) have been reported in the spectroscopic study of  $^{89}\text{Rb}$  decay by Kitching and Johns.<sup>7</sup> These levels, at 1031.88, 2007.54, 2280.0, 2570.14, 2707.20, 3227.9, and 3508.8 keV in this experiment, are well established by energy sums and  $\gamma$ - $\gamma$  coincidence information. The 2770-keV level reported by Kitching and Johns, however, cannot be established from the results of this work. The lowest four major excited levels can be identified with the 1031-, 2000-, 2266-, and 2558-keV levels found in the  $^{89}\text{Sr}(d, p)^{89}\text{Sr}$  reaction studies of Cosman, Enge, and Sperduto<sup>10</sup>. However, no reaction levels are found to correspond well with the highest three major excited levels.

The energy levels observed for the first time by spectroscopy at 2451.7, 3303.5, 3651.7, 3845.7, 3988.1, 4049.2, and 4093.7 keV are based on energy sums. The level at 4093.7 keV is established because the  $\gamma$  ray which depopulates that level could not populate the 1031.88-keV level without exceeding  $Q_\beta$ . The other six levels involve at least three transitions to or from other well established levels.

The excited levels at 1473.22, 1940.23, and 2058.0 keV are also observed in a study of  $^{89}\text{Rb}$  decay for the first time, and are based mainly on  $\gamma$  rays which are close in energy to intense  $\gamma$  rays in the  $^{89}\text{Kr}$  decay, or to strong  $\gamma$  rays and escape peaks in  $^{89}\text{Rb}$  decay. The 2058.0-keV level is supported by the coincidence observed between the 1025.28- and 1031.88-keV  $\gamma$  rays. The ground-state transition from the 2058.0-keV level was observed by carefully fitting the region of the 2570.14-

TABLE I. The photopeaks observed in  $^{89}\text{Rb}$  decay.

Energy- (keV)	Relative intensity <sup>a</sup>	Intensity (per 100 decays) <sup>b</sup>	Placement (keV)
118.29 ± 0.50	0.2 ± 0.1	0.01	2570–2451
205.74 ± 0.40 <sup>c</sup>	0.2 ± 0.1	0.01	3508–3303
272.45 ± 0.10	24.4 ± 1.2	1.6	2280–2007
289.76 ± 0.10	9.3 ± 0.5	0.59	2570–2280
466.62 ± 0.15 <sup>c</sup>	1.2 ± 0.3	0.073	1940–1473
562.50 ± 0.20	0.8 ± 0.1	0.05	2570–2007
595.96 ± 0.30	0.4 ± 0.1	0.03	3303–2707
657.71 ± 0.07	172 ± 9	10.9	3227–2570
699.62 ± 0.40	0.4 ± 0.1	0.03	2707–2007
766.79 ± 0.15	2.8 ± 0.3	0.18	2707–1940
776.19 ± 0.25 <sup>c</sup>	1.2 ± 0.3	0.073	3227–2451
801.08 ± 0.50	0.3 ± 0.2	0.02	3508–2707
822.03 ± 0.40	0.5 ± 0.2	0.03	4049–3227
947.69 ± 0.07	159 ± 8	10.1	3227–2280
975.32 ± 0.20	1.0 ± 0.2	0.062	2007–1031
1025.28 ± 0.50	3.9 ± 1.4	0.25	2058–1031
1031.88 ± 0.07	1000 ± 54	64.1	1031–0
1057.20 ± 0.40	0.4 ± 0.2	0.03	3508–2451
1081.43 ± 0.30	0.4 ± 0.1	0.03	3651–2570
1138.49 ± 0.50	0.2 ± 0.1	0.01	3845–2707
1160.47 ± 0.25	0.6 ± 0.1	0.04	
1211.70 ± 0.50	0.2 ± 0.1	0.01	
1220.32 ± 0.10	3.8 ± 0.3	0.24	3227–2007
1228.40 ± 0.15 <sup>c</sup>	2.1 ± 0.3	0.13	3508–2280
1234.02 ± 0.40	0.5 ± 0.3	0.03	2707–1473
1248.10 ± 0.07	734 ± 39	46.7	2280–1031
1419.57 ± 0.10	1.6 ± 0.2	0.098	2451–1031
1429.62 ± 0.50	0.2 ± 0.1	0.01	
1473.22 ± 0.20 <sup>c</sup>	6.1 ± 0.5	0.38	1473–0
1501.07 ± 0.20 <sup>c</sup>	3.4 ± 0.3	0.21	3508–2007
1538.08 ± 0.10	44 ± 3	2.8	2570–1031
1596.15 ± 0.50	0.3 ± 0.1	0.02	
1644.15 ± 0.30 <sup>c</sup>	0.4 ± 0.1	0.03	3651–2007
1770.20 ± 0.80	0.2 ± 0.1	0.01	4049–2280
1940.23 ± 0.30 <sup>c</sup>	5.7 ± 0.4	0.36	1940–0
1979.74 ± 0.50	0.4 ± 0.1	0.03	3988–2007
2007.54 ± 0.10	41 ± 3	2.6	2007–0
2058.00 ± 1.10	4.0 ± 1.5	0.25	2058–0
2109.74 ± 0.50	0.3 ± 0.1	0.02	4049–1940
2196.00 ± 0.15 <sup>c</sup>	230 ± 15	15.2	3227–1031
2231.29 ± 0.40	0.4 ± 0.1	0.03	
2280.06 ± 0.10 <sup>c</sup>	3.1 ± 0.3	0.20	2280–0
2372.77 ± 0.90	0.2 ± 0.1	0.01	3845–1473
2451.90 ± 0.20	0.9 ± 0.1	0.06	2451–0
2570.14 ± 0.10	170 ± 9	10.8	2570–0
2668.03 ± 0.50	0.2 ± 0.1	0.01	
2685.55 ± 0.40	0.5 ± 0.1	0.03	
2707.20 ± 0.10	35 ± 2	2.3	2707–0
2818.10 ± 0.50	0.2 ± 0.1	0.01	
2947.88 ± 0.40 <sup>c</sup>	0.3 ± 0.1	0.02	
2955.02 ± 1.20	0.1 ± 0.05	0.006	3988–1031
3037.49 ± 0.40	0.2 ± 0.1	0.01	
3141.66 ± 0.30 <sup>c</sup>	0.9 ± 0.1	0.06	
3227.88 ± 0.15	1.3 ± 0.1	0.083	3227–0
3263.63 ± 0.30	0.3 ± 0.1	0.02	
3303.54 ± 0.80	0.1 ± 0.05	0.006	3303–0
3508.84 ± 0.25	19.8 ± 1.2	1.3	3508–0
3651.75 ± 0.40	0.6 ± 0.2	0.04	3651–0
3781.80 ± 0.50	0.2 ± 0.1	0.01	

TABLE I (Continued)

Energy (keV)	Relative intensity <sup>a</sup>	Intensity (per 100 decays) <sup>b</sup>	Placement (keV)
3845.35 ± 0.60	0.5 ± 0.1	0.03	3845-0
3989.10 ± 0.80	0.3 ± 0.1	0.02	3988-0
4093.70 ± 0.60	1.3 ± 0.2	0.083	4093-0

<sup>a</sup> Measured relative to the 1031.88-keV transition.

<sup>b</sup> Calculated from the decay scheme of Fig. 1, and assuming a ground-state  $\beta$  branch of 18%.

<sup>c</sup> A photopeak with nearly the same energy appears in <sup>89</sup>Kr decay.

keV  $\gamma$ -ray single-escape peak. The 1940.23-keV level is based on the definite coincidence of the 1940.23- and 766.79-keV photopeaks. Possible coincidences between the 466.62-, 766.79-, and 1234.02-keV  $\gamma$  rays and the 1473.22-keV  $\gamma$  ray establish the 1473.22-keV level. The 1473.22- and 466.62-keV coincidence in <sup>89</sup>Rb decay is a factor of 30 too large to be accounted for by contamination from <sup>89</sup>Kr decay. These three levels correspond well in energy to levels reported in stripping experiments.<sup>10</sup>

#### C. Decay of <sup>89</sup>Kr

From the complex  $\gamma$ -ray spectrum of <sup>89</sup>Kr decay, 299 photopeaks are assigned to <sup>89</sup>Kr decay, of which 260 are placed in a level scheme for <sup>89</sup>Rb with 55 excited levels. The placement of 260  $\gamma$  rays accounts for 98.8% of the observed  $\gamma$ -ray intensity. The  $\gamma$  rays attributed to <sup>89</sup>Kr decay are summarized in Table III. As in the <sup>89</sup>Rb decay, the data obtained using the low-energy photon spectrometer revealed, within the 2% statistics of the data, that no  $\gamma$  rays below 197 keV and no <sup>89</sup>Rb x rays were present. A total of 105 coincidence gates in the <sup>89</sup>Kr decay were studied. Tabulated coincidence results are contained in Ref. 20. No attempt was made to resolve the 197- and 497-keV doublets, and the corresponding coincidence gates included information appropriate to both peaks in each doublet.

In the present work all levels except those at 3965.5, 4307.2, 4338.4, 4478.4, 4631.1, and 4685.9 keV have at least one piece of coincidence information to aid in their establishment. These six levels are based on at least three transitions to other well established levels. The <sup>89</sup>Rb level scheme is shown in Fig. 2 with transitions and coincidences indicated as in the <sup>89</sup>Sr level scheme. The four dashed levels in this scheme indicate that a lesser degree of confidence is placed in their establishment. For clarity in  $\gamma$ -ray placement, the level spacing in the <sup>89</sup>Rb level scheme is not necessarily proportional to the energy difference between levels.

A comparison can be made between excited levels in <sup>89</sup>Rb established in the present work and those found by Kitching and Johns<sup>17</sup> and by Poehlman.<sup>18</sup> The present work finds three excited levels below 2 MeV in <sup>89</sup>Rb not reported by Poehlman. These levels, at 1339.9, 1488.13, and 1864.7 keV, each have at least two supporting coincidences in the present work. In this work the 867.08- and 1533.68-keV  $\gamma$ -ray cascade is used to establish a level at 867.08 keV, while Poehlman bases a 1533.6-keV level on this cascade. It was found in the present experiment that the 867.08-keV  $\gamma$  ray is 15% more intense than the 1533.68-keV  $\gamma$  ray and, if a level is established at 1533.68 keV, no transitions are found which would aid in its depopulation. Thus the level is established at 867.08 keV. In addition, it is observed that the 2853.25-keV  $\gamma$  ray is in coincidence with the 867.08-keV transition, which would be impossible if the 867.08-keV transition fed a level at 1533.68 keV. There is no evidence in the present work

TABLE II. Percent  $\beta$  branching and  $\log ft$  values for <sup>89</sup>Rb decay.

<sup>89</sup> Sr level (keV)	$\beta$ group energy (MeV)	Percent $\beta$ branching	$\log f_0 t$
0.0	4.49	18 <sup>a</sup>	7.6
1031.88	3.45	~0	...
1473.22	3.01	0.25	8.7
1940.23	2.55	0.23	8.4
2007.54	2.48	0.48	8.0
2058.0	2.43	0.49	8.0
2280.0	2.21	37.2	6.0
2451.7	2.03	0.15	8.2
2570.14	1.92	3.25	6.8
2707.20	1.78	2.45	6.8
3227.9	1.26	36.2	5.0
3303.5	1.18	0.25	8.0
3508.8	0.98	1.67	6.0
3651.7	0.83	0.10	6.9
3845.7	0.64	0.05	6.8
3988.1	0.50	0.06	6.4
4049.2	0.44	0.06	6.1
4093.7	0.39	0.08	5.8

<sup>a</sup> From Kitching and Johns (Ref. 7).

TABLE III. The photopeaks observed in  $^{89}\text{Kr}$  decay.

Energy (keV)	Relative intensity <sup>a</sup>	Intensity (per 100 decays) <sup>b</sup>	Placement (keV)
196.24±0.50	10.6±5.4	0.24	1195-997
197.46±0.30	91.0±7.0	2.1	2598-2400
205.03±0.20 <sup>c</sup>	6.2±1.2	0.14	1693-1488
220.90±0.07	1000 ±56	22.5	220-0
242.20±1.10	0.6±0.4	0.01	2400-2160
264.11±0.10	33 ±2	0.74	1195-930
267.67±0.30	4.2±0.9	0.094	2866-2598
286.27±0.40	1.3±0.4	0.029	4367-4080
295.52±0.70	0.8±0.6	0.02	2160-1864
304.66±0.70	1.1±0.6	0.025	1998-1693
318.31±0.30	2.2±0.7	0.049	4367-4048
338.20±0.10	17.1±1.4	0.39	2160-1821
345.03±0.10	59 ±4	1.3	930-585
356.06±0.07	207 ±11	4.7	576-220
364.88±0.10	45 ±3	1.0	585-220
369.30±0.10	69 ±4	1.6	1693-1324
380.66±0.30	2.3±0.6	0.052	2781-2400
402.25±0.20	15.9±1.8	0.036	2400-1998
411.42±0.10	128 ±7	2.9	997-585
419.20±0.30	1.9±0.5	0.043	3017-2598
438.08±0.10	48 ±3	1.1	2598-2160
466.13±0.10 <sup>c</sup>	40 ±3	0.90	2160-1693
488.46±0.60	3.9±1.7	0.088	4631-4143
490.76±0.20	16.1±2.1	0.36	1488-997
497.51±0.30	332 ±27	7.5	497-0
498.60±0.40	57 ±10	1.3	1693-1195
523.53±0.40	1.7±0.6	0.038	2387-1864
542.19±0.50	1.5±0.6	0.034	4685-4143
546.93±0.50	1.5±0.6	0.034	4080-3532
557.30±0.20	8.0±0.8	0.18	1488-930
576.96±0.10	282 ±16	6.3	576-0
585.80±0.07	826 ±45	18.6	585-0
599.52±0.20	4.4±0.6	0.099	2598-1998
610.17±0.70	0.9±0.5	0.02	1195-585
626.20±0.10	30 ±2	0.68	1821-1195
629.75±0.20	17.1±1.3	0.39	2160-1530
652.60±0.50	1.9±0.7	0.043	3250-2598
660.53±0.60	2.4±0.8	0.054	
662.86±0.40	3.9±0.9	0.088	1530-867
665.72±0.20	5.7±0.8	0.13	4631-3965
668.61±0.60	2.1±0.7	0.047	1864-1195
671.40±0.20	5.3±1.0	0.12	2365-1693
674.11±0.20	11.6±1.1	0.26	1998-1324
687.31±0.40	3.5±0.9	0.079	4048-3361
696.24±0.10	89 ±6	2.0	1693-997
707.01±0.20	24.9±1.7	0.56	2400-1693
710.05±0.20	39 ±3	0.88	930-220
729.63±0.20	14.8±1.6	0.33	3327-2598
738.39±0.07	210 ±11	4.7	1324-585
747.39±0.30	5.7±1.3	0.13	1324-576
753.54±0.40	4.6±1.2	0.10	1339-585
762.87±0.30	20.0±4.0	0.45	1339-576
	46 ±6	1.0	1693-930
776.49±0.20 <sup>c</sup>	56 ±9	1.3	997-220
783.47±0.90	1.1±0.7	0.025	2781-1998
826.75±0.10	38 ±3	0.86	1324-497
835.53±0.10	55 ±4	1.2	2160-1324
857.37±0.15	14.3±1.2	0.32	3017-2160
867.08±0.07	296 ±15	6.7	867-0

TABLE III (Continued)

Energy (keV)	Relative intensity <sup>a</sup>	Intensity (per 100 decays) <sup>b</sup>	Placement (keV)
870.42 ± 0.20	8.0 ± 0.9	0.18	2400-1530
904.27 ± 0.07	359 ± 20	8.1	2598-1693
917.78 ± 0.20	3.7 ± 0.6	0.083	2781-1864
930.95 ± 0.10	31 ± 2	0.70	930-0
934.61 ± 0.50	1.9 ± 0.6	0.043	1864-930
939.44 ± 0.30	3.3 ± 0.7	0.074	4405-3465
944.19 ± 0.15	8.2 ± 0.8	0.18	1530-585
953.18 ± 0.20	5.3 ± 0.8	0.12	1530-576
960.42 ± 0.10	16.1 ± 1.3	0.36	3361-2400
964.15 ± 0.40	2.9 ± 0.7	0.065	2160-1195
969.73 ± 0.30	4.7 ± 0.7	0.11	3370-2400
974.39 ± 0.10	49 ± 3	1.1	1195-220
997.37 ± 0.10	33 ± 2	0.74	997-0
1010.84 ± 0.20	5.4 ± 0.7	0.12	4338-3327
1038.28 ± 0.50	1.5 ± 0.6	0.034	
1044.40 ± 0.10	20.4 ± 1.4	0.46	2866-1821
1048.23 ± 0.30	3.1 ± 0.6	0.070	2387-1339
1058.62 ± 0.80	1.5 ± 0.8	0.034	3327-2269
1063.05 ± 0.40	3.5 ± 0.8	0.079	2387-1324
1067.74 ± 0.40	3.4 ± 0.8	0.076	1998-930
1076.48 ± 0.20	11.8 ± 1.3	0.27	2400-1324
1088.07 ± 0.10	17.9 ± 1.6	0.40	2781-1693
1098.06 ± 0.50	3.2 ± 1.2	0.072	4631-3532
1103.18 ± 0.20	45 ± 3	1.0	1324-220
1107.78 ± 0.10	146 ± 9	3.3	1693-585
1116.61 ± 0.07	83 ± 5	1.9	1693-576
1131.51 ± 0.20	8.0 ± 1.1	0.18	1998-867
1152.24 ± 0.40	3.2 ± 0.8	0.072	3017-1864
1162.50 ± 0.10	10.7 ± 1.0	0.24	2160-997
1167.41 ± 0.60	1.7 ± 0.7	0.038	3327-2160
1172.33 ± 0.20	49 ± 4	1.1	2866-1693
1182.38 ± 0.20	8.3 ± 1.1	0.19	4048-2866
1186.54 ± 0.20	9.2 ± 0.9	0.21	3327-2140
1195.14 ± 0.30	4.2 ± 0.7	0.094	1195-0
1200.59 ± 1.10	0.9 ± 0.6	0.02	3361-2160
1210.24 ± 0.90	1.1 ± 0.7	0.025	3370-2160
1228.84 ± 0.30 <sup>c</sup>	7.2 ± 0.9	0.16	2160-930
1235.62 ± 0.10	29.7 ± 2.3	0.67	1821-585
1241.51 ± 0.40	4.4 ± 0.8	0.099	
1251.00 ± 0.70	1.9 ± 0.8	0.043	2781-1530
1267.16 ± 0.60	1.2 ± 0.9	0.027	1488-220
1273.73 ± 0.10	68 ± 4	1.5	2598-1324
1278.50 ± 0.80	1.6 ± 0.9	0.036	1864-585
1298.01 ± 0.50	2.2 ± 0.7	0.049	4080-2781
1302.65 ± 0.30	5.0 ± 0.7	0.11	4631-3327
1308.90 ± 0.30	3.4 ± 0.7	0.076	1530-220
1324.28 ± 0.07	153 ± 9	3.4	1324-0
1335.39 ± 0.30	6.6 ± 1.3	0.15	2866-1530
1340.63 ± 0.30	9.7 ± 1.2	0.22	1339-0
1367.48 ± 0.20	7.4 ± 0.9	0.17	1864-497
1372.16 ± 0.20	6.3 ± 0.8	0.14	3370-1998
1381.91 ± 0.50	2.9 ± 0.8	0.065	4631-3250
1412.59 ± 0.15	13.2 ± 1.1	0.30	1998-585
1421.64 ± 0.20	11.2 ± 1.0	0.25	1998-576
1441.25 ± 0.80	1.0 ± 0.5	0.022	4307-2866
1455.31 ± 0.70	2.6 ± 1.1	0.058	
1458.32 ± 0.70	3.7 ± 1.2	0.083	2781-1324
1461.28 ± 0.50	6.1 ± 1.2	0.14	4478-3017
1464.24 ± 0.30	8.9 ± 1.2	0.20	2788-1324
1468.52 ± 0.30	9.4 ± 1.3	0.21	4487-3017

TABLE III (Continued)

Energy (keV)	Relative intensity <sup>a</sup>	Intensity (per 100 decays) <sup>b</sup>	Placement (keV)
1472.76 ± 0.10 <sup>c</sup>	344 ± 19	7.7	1693-220
1481.92 ± 0.60	2.2 ± 1.0	0.049	4080-2598
1488.13 ± 0.40	4.7 ± 1.0	0.11	1488-0
1500.96 ± 0.10 <sup>c</sup>	66 ± 5	1.5	1998-497
1506.15 ± 0.30	5.6 ± 1.0	0.13	3327-1821
1530.04 ± 0.15	166 ± 10	3.7	1530-0
1533.68 ± 0.15	256 ± 14	5.8	2400-867
1555.28 ± 0.20	7.6 ± 0.9	0.17	2140-585
1573.78 ± 0.20	9.5 ± 0.9	0.21	2160-585
1582.87 ± 0.30	4.5 ± 0.7	0.10	2160-576
1600.71 ± 0.30	3.6 ± 0.7	0.081	1821-220
1634.06 ± 0.10	41 ± 3	0.92	3327-1693
1643.82 ± 0.10 <sup>c</sup>	16.9 ± 1.3	0.38	1864-220
1657.63 ± 0.50	2.0 ± 0.6	0.045	
1667.51 ± 0.20	6.4 ± 0.7	0.14	3361-1693
1676.91 ± 0.30	7.0 ± 1.1	0.16	3370-1693
1680.26 ± 0.50	4.2 ± 1.0	0.094	4080-2400
1683.82 ± 0.40	6.6 ± 1.2	0.15	2269-585
1692.00 ± 1.20	12.8 ± 5.1	0.29	3017-1324
1693.70 ± 0.10	219 ± 14	4.9	1693-0
1707.92 ± 0.80	1.2 ± 0.5	0.027	3977-2269
1710.70 ± 0.60	1.7 ± 0.6	0.038	3532-1821
1721.29 ± 0.15	11.2 ± 0.9	0.25	2218-497
1729.92 ± 0.60	1.5 ± 0.6	0.034	
1735.50 ± 0.40	2.8 ± 0.6	0.063	
1766.10 ± 0.40	2.4 ± 0.6	0.054	4631-2866
1777.60 ± 0.10	38 ± 3	0.86	1998-220
1788.24 ± 0.30	5.3 ± 0.8	0.12	2365-576
1791.35 ± 0.60	2.3 ± 0.7	0.052	2788-997
1804.41 ± 0.60	1.5 ± 0.6	0.034	
1810.73 ± 0.20	7.0 ± 0.8	0.16	2387-576
1823.61 ± 0.40	3.3 ± 0.7	0.074	2400-576
1827.30 ± 0.40	3.2 ± 0.6	0.072	
1831.30 ± 0.30	4.3 ± 0.6	0.097	3361-1530
1837.47 ± 0.40	5.9 ± 1.4	0.13	
1839.72 ± 0.25	17.5 ± 1.7	0.39	3327-1488
1850.57 ± 0.40	2.5 ± 0.6	0.056	2781-930
1865.24 ± 0.50	4.0 ± 0.7	0.090	1864-0
1868.47 ± 0.25	9.8 ± 0.9	0.22	2866-997
1879.80 ± 0.25	7.9 ± 0.8	0.18	4478-2598
1886.50 ± 0.60	1.7 ± 0.6	0.038	
1897.83 ± 0.70	1.5 ± 0.6	0.034	3719-1821
1903.40 ± 0.10	52 ± 5	1.2	2400-497
1925.31 ± 0.90	0.8 ± 0.6	0.02	3250-1324
1935.11 ± 0.60	1.7 ± 0.6	0.038	2866-930
1939.11 ± 0.15 <sup>c</sup>	32 ± 2	0.72	2160-220
1966.55 ± 0.20	6.6 ± 0.7	0.15	4367-2400
1977.70 ± 0.50	1.9 ± 0.6	0.043	3465-1488
1998.63 ± 0.50	5.9 ± 1.1	0.13	1998-0
2001.63 ± 0.90	1.8 ± 0.8	0.040	3532-1530
2012.23 ± 0.10	78 ± 5	1.8	2598-585
2021.04 ± 0.15	12.2 ± 1.0	0.27	2598-576
2039.48 ± 1.00	0.9 ± 0.5	0.02	4405-2365
2046.47 ± 0.15	13.1 ± 1.0	0.30	3370-1324
2079.29 ± 0.90	1.5 ± 0.6	0.034	
2082.47 ± 0.50	2.9 ± 0.7	0.065	4080-1998
2100.63 ± 0.08	47 ± 3	1.1	2598-497
2140.47 ± 0.60	3.1 ± 0.6	0.070	2140-0
2143.83 ± 0.40	3.2 ± 0.6	0.072	3965-1821



TABLE III (Continued)

Energy (keV)	Relative intensity <sup>a</sup>	Intensity (per 100 decays) <sup>b</sup>	Placement (keV)
2150.11±0.80	1.0±0.6	0.022	3017-867
2160.02±0.09	26.4±1.8	0.59	2160-0
2167.90±0.60	2.1±0.7	0.047	
2189.98±0.90	1.3±0.7	0.029	3719-1530
2195.76±0.40 <sup>c</sup>	6.4±2.7	0.14	2781-585
2207.17±0.50	2.3±0.7	0.052	4367-2160
2232.55±0.80	1.2±0.5	0.027	4230-1998
2280.22±0.30 <sup>c</sup>	10.2±2.0	0.23	2866-585
2285.59±0.80	2.3±1.0	0.052	4685-2400
2321.65±0.50	2.6±0.7	0.058	4143-1821
2329.99±0.80	1.8±0.7	0.040	3327-997
2377.38±0.90	40 ±3	0.90	2598-220
2400.99±0.09	36 ±3	0.81	2400-0
2440.91±0.40	2.3±0.8	0.052	3017-576
2467.30±1.10	0.8±0.5	0.02	3465-997
2487.82±0.80	1.2±0.5	0.027	4631-2140
2503.02±0.50	2.5±0.6	0.056	3370-867
2522.03±0.50	2.5±0.6	0.056	3717-1195
2534.94±0.30	4.7±0.7	0.11	3532-997
2545.44±0.60	2.5±0.7	0.056	4367-1821
2549.85±0.90	1.5±0.6	0.034	4080-1530
2555.27±0.80	1.7±0.6	0.038	
2597.92±0.20	5.4±0.8	0.12	2598-0
2622.82±1.00	1.1±0.6	0.025	4487-1864
2645.26±0.15	21.0±1.5	0.47	2866-220
2659.08±0.50	4.3±0.8	0.097	
2703.23±0.90	1.7±0.7	0.038	
2721.91±0.70	1.8±0.7	0.040	3721-997
2742.33±0.80	1.4±0.6	0.031	3327-585
2750.92±0.30	6.2±0.7	0.14	3327-576
2756.60±0.50	3.3±0.7	0.074	4080-1324
2760.27±0.70	2.3±0.8	0.052	
2775.74±1.10	1.5±1.0	0.034	3361-585
2782.11±0.10	38 ±3	0.86	2781-0
2789.18±0.60	2.6±0.9	0.058	2788-0
2793.75±0.20	34 ±2	0.77	3370-576
2804.13±0.80	2.0±0.8	0.045	
2819.58±0.25	6.6±0.8	0.15	4143-1324
2853.25±0.30	12.0±1.7	0.27	3719-867
2866.23±0.10	87 ±5	2.0	2866-0
2873.79±0.40	4.8±0.9	0.11	3370-497
2878.69±0.25	16.2±1.5	0.36	3465-585
2917.37±0.70	1.5±0.5	0.034	4405-1488
2946.89±0.40 <sup>c</sup>	3.9±0.7	0.088	3532-585
2998.40±0.60	2.2±0.6	0.049	4487-1488
3017.92±0.30	12.7±1.4	0.29	3017-0
3029.16±0.25	13.5±1.2	0.30	3250-220
3049.72±0.70	2.0±0.6	0.045	
3098.75±0.70	1.9±0.6	0.043	3965-867
3107.26±0.25	9.7±0.9	0.22	3327-220
3140.26±0.20 <sup>c</sup>	52 ±4	1.2	3717-576
3154.36±1.00	1.3±0.7	0.029	4478-1324
3159.84±0.60	3.1±0.6	0.070	
3172.09±0.30	5.0±0.7	0.11	4367-1195
3213.24±0.90	1.6±0.6	0.036	4143-930
3219.84±0.20	21.4±1.6	0.48	3717-497
3257.02±0.50	2.6±0.6	0.058	3834-576
3271.30±0.50	2.7±0.6	0.061	

TABLE III (Continued)

Energy (keV)	Relative intensity <sup>a</sup>	Intensity (per 100 decays) <sup>b</sup>	Placement (keV)
3300.01 ± 0.60	1.9 ± 0.6	0.043	4230-930
3317.86 ± 0.60	4.1 ± 0.9	0.092	
3321.93 ± 0.50	3.5 ± 0.8	0.079	3898-576
3340.82 ± 0.90	1.8 ± 0.7	0.040	4338-997
3347.44 ± 0.60	3.4 ± 0.8	0.076	
3351.94 ± 0.90	2.1 ± 0.7	0.047	
3361.70 ± 0.20	52 ± 4	1.2	3361-0
3371.12 ± 0.35	31 ± 3	0.70	3370-0
3399.88 ± 0.30	6.8 ± 0.7	0.15	3977-576
3439.57 ± 0.60	2.2 ± 0.6	0.049	4307-867
3463.26 ± 1.20	2.1 ± 1.2	0.047	4048-585
3503.60 ± 1.40	1.0 ± 0.6	0.022	4080-576
3532.88 ± 0.20	67 ± 4	1.5	3532-0
3567.91 ± 0.70	2.8 ± 0.9	0.063	
3583.90 ± 0.30	12.9 ± 1.0	0.29	4080-497
3629.22 ± 0.50	4.0 ± 0.7	0.090	
3634.39 ± 0.90	1.9 ± 0.6	0.043	4631-997
3639.05 ± 0.80	1.9 ± 0.6	0.043	4216-576
3652.34 ± 0.50	2.9 ± 0.6	0.065	
3665.40 ± 0.40	4.2 ± 0.6	0.094	
3677.74 ± 0.40	3.3 ± 0.6	0.074	3898-220
3717.76 ± 0.40	42 ± 3	0.94	3717-0
3721.45 ± 0.90	2.4 ± 1.0	0.054	4307-585
3732.51 ± 0.60	6.9 ± 2.5	0.16	4230-497
3756.54 ± 1.30	0.8 ± 0.5	0.02	3977-220
3781.43 ± 0.40	6.6 ± 0.6	0.15	4367-585
3809.51 ± 0.80	1.0 ± 0.4	0.022	4307-497
3827.42 ± 0.40	6.9 ± 0.8	0.16	4048-220
3837.57 ± 0.50	4.1 ± 0.5	0.092	
3842.73 ± 0.40	5.5 ± 0.6	0.12	4340-497
3882.48 ± 0.60	2.0 ± 0.4	0.045	
3898.42 ± 1.00	1.7 ± 0.9	0.038	3898-0
3901.66 ± 0.40	6.7 ± 1.0	0.15	4487-585
3923.02 ± 0.40	20.7 ± 1.4	0.47	4143-220
3965.53 ± 0.40	10.4 ± 0.8	0.23	3965-0
3977.54 ± 0.40	3.5 ± 0.6	0.079	4198-220
	13.5 ± 2.5	0.30	3977-0
3995.96 ± 0.40	7.1 ± 0.6	0.16	4216-220
4004.88 ± 0.70	1.4 ± 0.4	0.031	
4043.75 ± 1.00	1.0 ± 0.4	0.022	4631-585
4048.04 ± 0.50	5.8 ± 0.6	0.13	4048-0
4081.42 ± 0.50	3.7 ± 0.5	0.083	4080-0
4117.67 ± 1.10	0.7 ± 0.3	0.02	4338-220
4142.98 ± 1.20	1.3 ± 0.4	0.029	4143-0
4146.88 ± 1.30	0.8 ± 0.4	0.02	4367-220
4162.61 ± 0.60	1.4 ± 0.3	0.031	
4176.20 ± 1.10	0.6 ± 0.3	0.01	
4184.27 ± 0.60	2.5 ± 0.4	0.056	4405-220
4253.28 ± 1.00	0.7 ± 0.3	0.02	
4267.70 ± 0.60	1.4 ± 0.3	0.031	4487-220
4279.36 ± 0.70	1.0 ± 0.3	0.022	
4307.36 ± 1.10	0.5 ± 0.3	0.01	4307-0
4321.23 ± 1.10	0.5 ± 0.2	0.01	
4341.13 ± 0.60	5.2 ± 0.5	0.12	4340-0
4368.36 ± 0.75	2.1 ± 0.3	0.047	4367-0
4405.08 ± 1.20	0.4 ± 0.2	0.01	4405-0
4448.07 ± 1.20	0.5 ± 0.2	0.01	
4478.25 ± 0.90	0.7 ± 0.2	0.02	4478-0
4489.19 ± 0.80	6.7 ± 0.6	0.15	4487-0

TABLE III (Continued)

Energy (keV)	Relative intensity <sup>a</sup>	Intensity (per 100 decays) <sup>b</sup>	Placement (keV)
4631.49 ± 0.80	1.4 ± 0.3	0.031	4631-0
4655.57 ± 0.70	0.5 ± 0.2	0.01	
4685.64 ± 1.20	0.4 ± 0.2	0.01	4685-0
4701.51 ± 0.90	0.5 ± 0.2	0.01	

<sup>a</sup> Measured relative to the 220.90-keV transition.

<sup>b</sup> Calculated from the decay scheme of Fig. 2, a <sup>89</sup>Rb and <sup>89</sup>Kr equilibrium measurement, and assuming a ground-state  $\beta$  branch of 18% for <sup>89</sup>Rb.

<sup>c</sup> A photopeak with nearly the same energy appears in <sup>89</sup>Rb decay.

for a doublet level at 930.7 and 931.5 keV as found by Poehlman, or for a level at 1760 keV as found by Kitching and Johns. Above 2 MeV, the present work and that of Poehlman are in agreement on the main levels. However, they disagree in many of the levels involving fewer and less intense  $\gamma$  rays.

The percent  $\beta$  feeding to each <sup>89</sup>Rb level and the corresponding  $\log ft$  value, summarized in Table IV, were calculated in the same manner as those for <sup>89</sup>Sr. Using the completed level schemes for <sup>89</sup>Rb and <sup>89</sup>Sr and the equilibrium data accumulation, the ground-state  $\beta$  branch from <sup>89</sup>Kr decay was determined to be (14 ± 2)%. This result, combined with the  $Q_\beta$  value of 4.93 ± 0.06 MeV reported by Clifford,<sup>21</sup> was used in the  $\log ft$  calculations. In this work, it was also found that no  $\beta$  feeding occurred to the 220.90-keV level, within errors of the experiment. The  $Q_\beta$  value of 5.15 ± 0.03 MeV for <sup>89</sup>Kr decay reported by Kitching and Johns<sup>17</sup> is based upon 0.1% ground-state  $\beta$  feeding and 4%  $\beta$  feeding to the 220.90-keV level. The present work supports the 4.93 ± 0.06-MeV  $Q_\beta$  value, which assumed no  $\beta$  feeding to the 220.90-keV level, and is derived from  $\gamma$ -gated  $\beta$  spectra for seven gating transitions.

#### IV. DISCUSSION

##### A. <sup>89</sup>Sr Level Scheme

As previously mentioned, the <sup>89</sup>Sr nucleus has been studied extensively, both experimentally and theoretically. In particular, the positive-parity levels seem well understood in terms of the positive-parity neutron single-particle levels above the  $N=50$  closed shell and the coupling of these levels to the 2<sub>1</sub><sup>+</sup> quadrupole first excited state of <sup>88</sup>Sr.<sup>10,14,15</sup> The negative-parity levels, however, are not as well understood, but could correspond to a coupling of the positive-parity neutron states to the 3<sup>-</sup> octupole state of <sup>88</sup>Sr.<sup>10,15</sup> These negative-parity states are important to the understanding

of this level scheme since 73% of the  $\beta$  decay of <sup>89</sup>Rb occurs to the 2280.0- and 3227.9-keV levels, which are assigned negative parity on the basis of  $\beta$ -branch  $\log ft$  values.

Before examining the 2280.0- and 3227.9-keV levels, consider the ground state of <sup>89</sup>Rb and the ground state and first excited state of <sup>89</sup>Sr. On

TABLE IV. Percent  $\beta$  branching and  $\log ft$  values for <sup>89</sup>Kr decay.

<sup>89</sup> Rb levels (keV)	Percent $\beta$ branching	$\log f_0 t$ <sup>a</sup>	<sup>89</sup> Rb levels (keV)	Percent $\beta$ branching	$\log f_0 t$
0.0	14	7.2	3250.1	0.30	6.9
220.90	~0	...	3327.1	2.2	5.9
497.5	1.2	8.1	3361.7	1.8	6.0
576.96	4.3	7.5	3370.9	2.6	5.8
585.80	2.6	7.7	3465.0	0.35	6.6
867.08	0.19	8.7	3532.8	1.7	5.8
930.95	0.51	8.2	3717.5	2.7	5.3
997.35	1.5	7.7	3719.8	0.38	6.2
1195.2	~0	...	3834.0	0.58	5.8
1324.28	4.0	7.1	3898.6	0.19	6.2
1339.9	0.70	7.9	3965.5	0.22	6.1
1488.13	~0	...	3977.5	0.50	5.7
1530.04	3.2	7.1	4048.6	0.56	5.5
1693.70	11	6.5	4080.6	0.77	5.3
1821.4	0.25	8.0	4143.6	0.62	5.3
1864.7	0.52	7.7	4198.4	0.08	6.0
1998.5	2.3	7.0	4216.4	0.20	5.6
2140.8	~0	...	4230.9	0.23	5.5
2160.02	3.2	6.7	4307.2	0.16	5.5
2218.8	0.25	7.8	4338.4	0.18	5.4
2269.6	0.09	8.2	4340.6	0.24	5.2
2365.2	0.22	7.7	4367.3	0.66	4.7
2387.9	0.35	7.5	4405.0	0.19	5.2
2400.99	6.3	6.3	4478.4	0.40	4.6
2598.1	17	5.7	4487.7	0.62	4.4
2781.7	1.7	6.5	4631.1	0.67	3.8
2788.8	0.31	7.3	4685.9	0.10	4.4
2866.2	4.5	6.0			
3017.9	0.74	6.7			

<sup>a</sup> Calculated using a  $Q$  value of 4.93 MeV.

the basis of shell-model states, the  $^{89}\text{Rb}$  ground state is either  $\pi(2p_{3/2})^{-1}$  or  $\pi(1f_{5/2})^{-1}$ . A survey of rubidium isotopes<sup>22</sup> suggests that the  $^{89}\text{Rb}$  ground-state spin and parity is  $\frac{3}{2}^{-}$ , consistent with a  $\pi(2p_{3/2})^{-1}$  configuration. Additionally, if a  $2d_{5/2}$  neutron is coupled to the  $^{89}\text{Rb}$  ground state calculated by Vergados,<sup>16</sup> with large  $\pi(2p_{3/2})^{-1}\nu(2d_{5/2})$  and smaller  $\pi(1f_{5/2})^{-1}\nu(2d_{5/2})$  and  $\pi(2p_{3/2})^{-1}\nu(3s_{1/2})$  components being the most important, most of the  $^{89}\text{Rb}$  ground-state configuration would be  $\pi(2p_{3/2})^{-1}$ , supporting a  $J^{\pi}$  of  $\frac{3}{2}^{-}$ . A  $^{89}\text{Sr}$  ground-state spin and parity of  $\frac{5}{2}^{+}$  is consistent with the first-forbidden unique  $\beta$  decay observed to the  $\frac{1}{2}^{-}$   $^{89}\text{Y}$  ground state,<sup>23</sup> and is further supported in reaction studies.<sup>10-12</sup> This  $J^{\pi}$  assignment is in agreement with a predicted ground-state configuration for  $^{89}\text{Sr}$  of a  $2d_{5/2}$  neutron coupled to a closed  $^{88}\text{Sr}$  core in the shell-model picture. Vergados<sup>16</sup> calculated that about 90% of the  $^{89}\text{Sr}$  ground state is  $\nu(2d_{5/2})$  with most of the rest consisting of a number of small components of proton and neutron particle-hole states coupled to the  $2d_{5/2}$  neutron. The 18%  $\beta$  branch from  $^{89}\text{Rb}$  to the  $^{89}\text{Sr}$  ground state, and the resulting  $\log ft$  value of 7.6, are consistent with a nonunique first-forbidden  $\beta$  transition involving the decay of a  $2d_{5/2}$  neutron into a  $2p_{3/2}$  or  $1f_{5/2}$  proton.

Reaction studies<sup>10,13</sup> suggest that the 1031.88-

keV first excited level in  $^{89}\text{Sr}$  is composed largely of a  $3s_{1/2}$  neutron coupled to the  $^{88}\text{Sr}$  closed core.  $\beta$  decay to this level from the  $^{89}\text{Rb}$  ground state, consisting mainly of the  $\pi(2p_{3/2})^{-1}\nu(2d_{5/2})^2$  component, would be inhibited because two-body processes in the  $\beta$  decay would then have to be invoked. The absence of a  $\beta$  branch to the 1031.88-keV first excited level as determined in this work is thus consistent with a  $\nu(3s_{1/2})$  single-particle configuration for this level. The  $\gamma$ -ray transition between the 1031.88-keV level and the ground state would then be a single-particle  $E2$  transition.

The  $\beta$ -decay branch to the 2280.0-keV level has a  $\log ft$  value of 6.0, indicating an allowed  $\beta$  transition. An intense  $\gamma$  ray to the  $\nu(3s_{1/2})$  1031.88-keV level and a weak transition to the  $\nu(2d_{5/2})$  ground state suggest a state configuration composed mainly of the  $3s_{1/2}$  neutron coupled to the  $3^{-}$  state of  $^{88}\text{Sr}$  with  $J^{\pi}$  of  $\frac{5}{2}^{-}$ , instead of the  $\nu(2d_{5/2}) \otimes 3^{-}$  configuration suggested by Hughes.<sup>15</sup> The transition between the 2280.0- and 1031.88-keV levels would then be collective  $E3$ , while the transition between the 2280.0-keV level and the ground state would be particle-inhibited  $E1$  or  $E3$ . If it is assumed that both transitions are  $E3$ , about 1% admixture of the  $\nu(2d_{5/2}) \otimes 3^{-}$  configuration could be allowed in the 2280.0-keV state. The 37%  $\beta$  feeding to the 2280.0-keV level can be explained

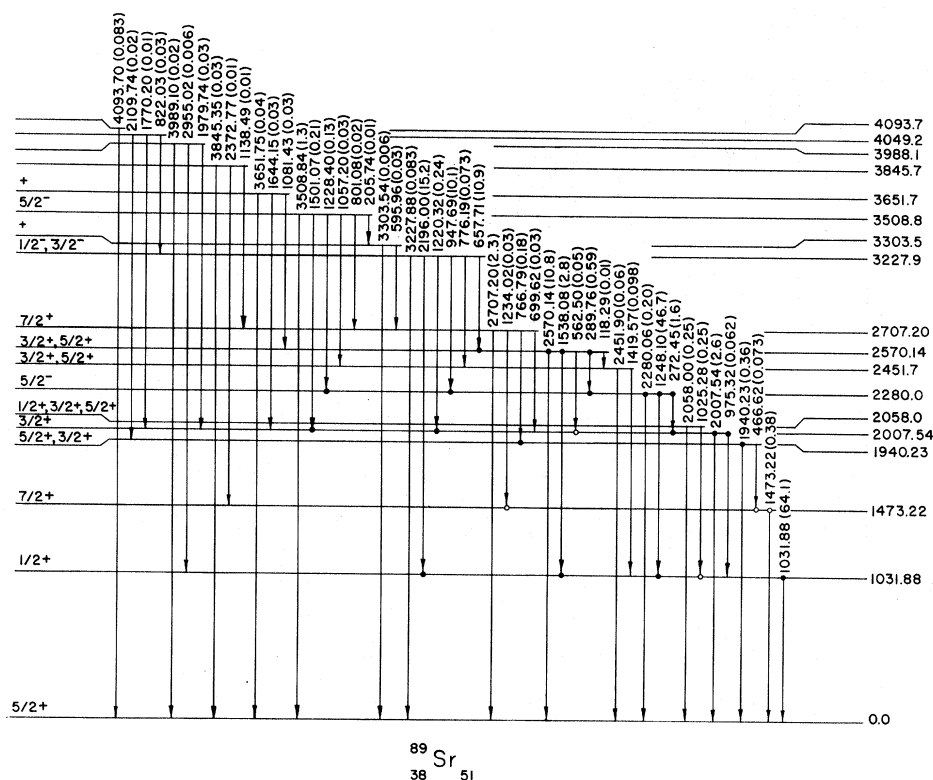


FIG. 1. The  $^{89}\text{Sr}$  level scheme with  $J^{\pi}$  assignments.

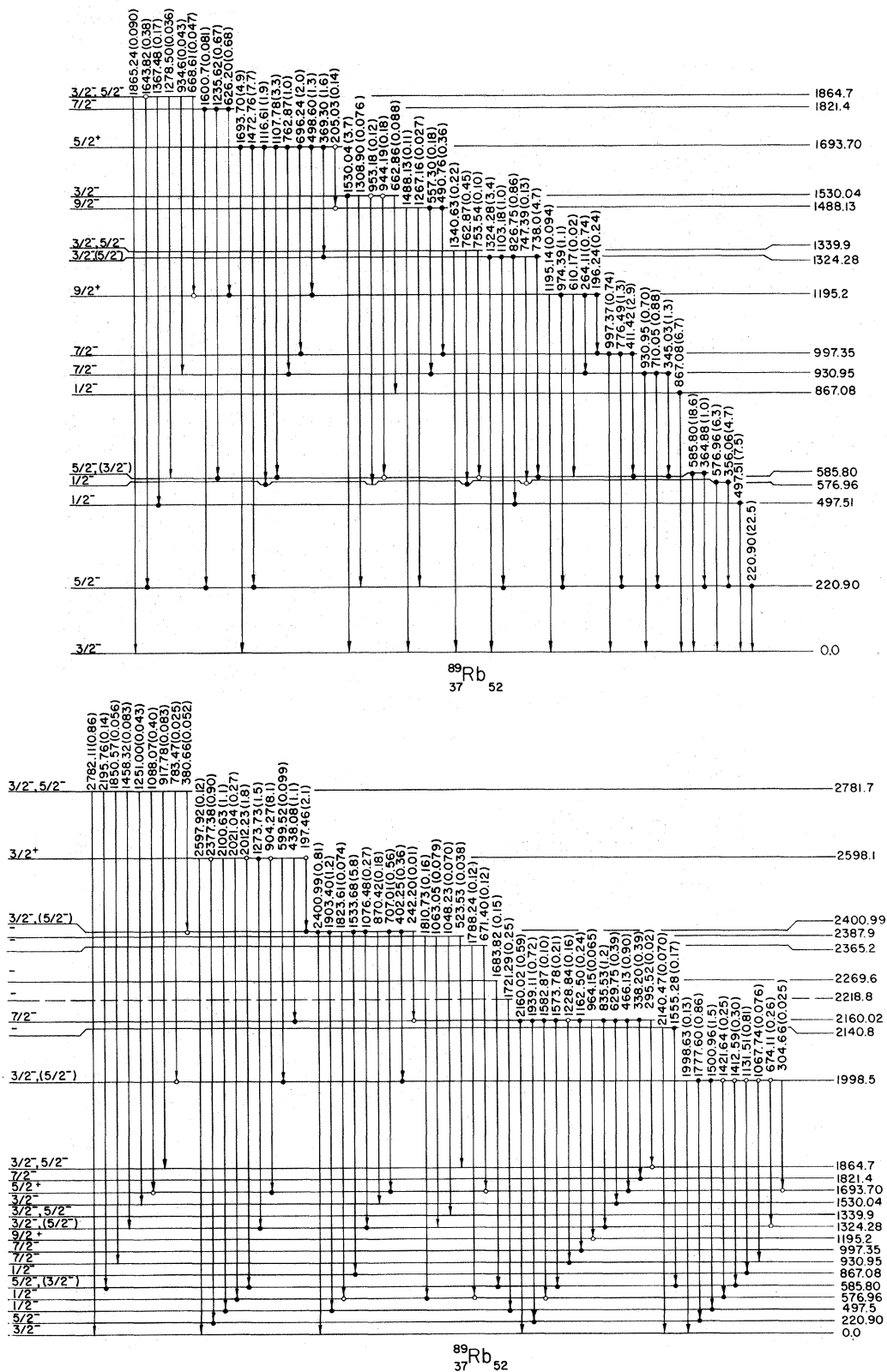


FIG. 2. The  $^{89}\text{Rb}$  level scheme with tentative  $J^\pi$  assignments.

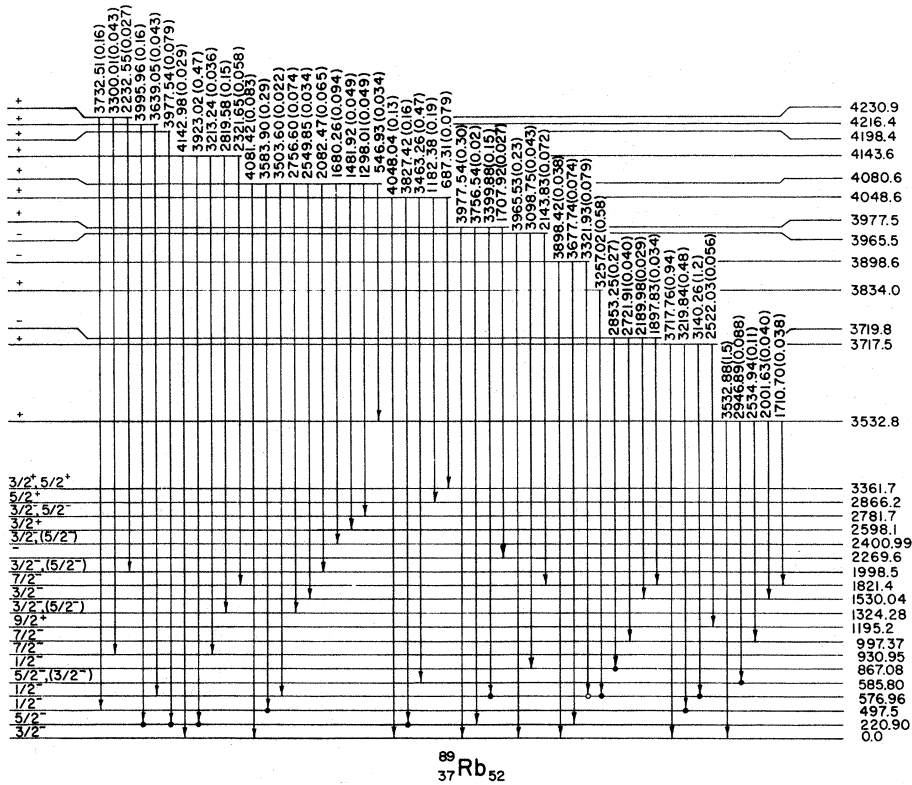
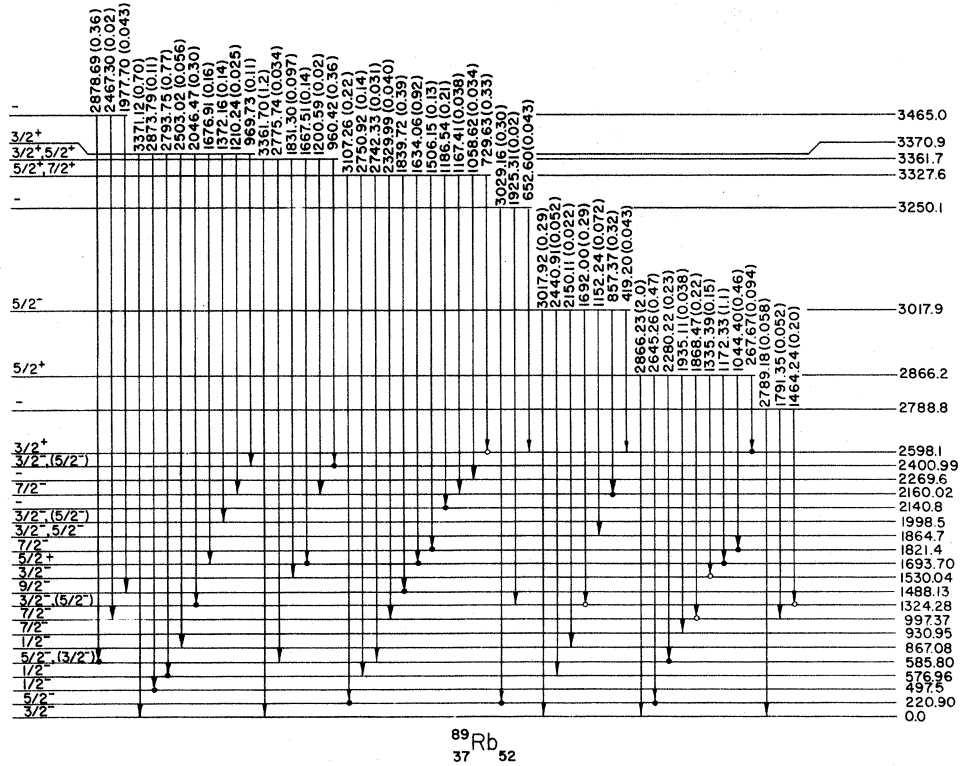


FIG. 2 (Continued)

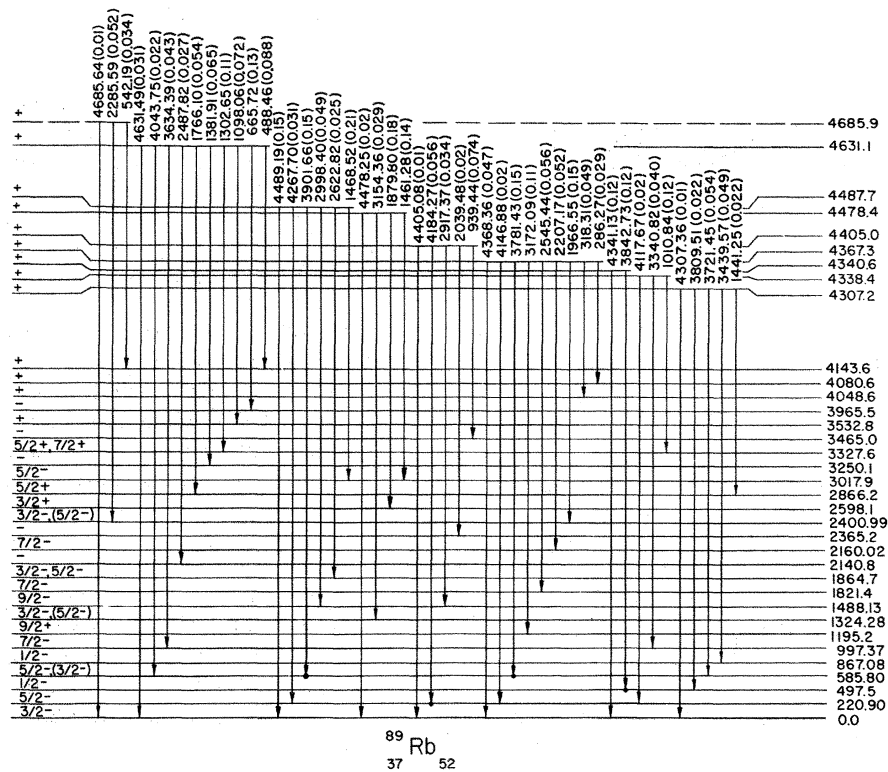


FIG. 2 (Continued)

on the basis of this suggested configuration. Shastry<sup>24</sup> calculates that the  $^{88}\text{Sr}$   $3^-$  state is composed mainly of the  $\pi(2p_{3/2})^{-1}(1g_{9/2})$  configuration with smaller  $\pi(2p_{3/2})^{-1}(2d_{5/2})$  and  $\pi(2p_{3/2})^{-1}(1g_{7/2})$  contributions and many other still smaller proton particle-hole contributions. Comparison of the 2280.0-keV level wave function formed by coupling the  $\nu(3s_{1/2})$  configuration [plus a  $\nu(2d_{5/2})$  admixture] to the calculated  $^{88}\text{Sr}$   $3^-$  configuration with the  $^{89}\text{Rb}$  ground-state wave function suggested above shows Fermi  $\beta$ -decay matrix elements are possible between certain components of these wave functions. Though these components account for only a small part of the particle-hole expansions of the involved wave functions, the  $\beta$ -transition matrix elements between them are of the superallowed type, since no particle has to change its substate. These important matrix elements contributing to this  $\beta$ -decay transition are given by

$$\langle \pi(2p_{3/2})^{-1}\pi(2d_{5/2})\nu(3s_{1/2}) | T_f | \pi(2p_{3/2})^{-1}\nu(2d_{5/2})\nu(3s_{1/2}) \rangle$$

and

$$\langle \pi(2p_{3/2})^{-1}\pi(2d_{5/2})\nu(2d_{5/2}) | T_f | \pi(2p_{3/2})^{-1}\nu(2d_{5/2})^2 \rangle,$$

where  $T_f$  is the Fermi  $\beta$ -decay operator.

From the  $^{89}\text{Sr}$  level scheme it is seen that the 3227.9-keV level is much like the 2280.0-keV level

in its characteristics and that the  $\beta$  transition to the 3227.9-keV level has a  $\log ft$  value of 5.0. Strong  $\gamma$ -ray transitions to the 2280.0- and 1031.88-keV levels and a weak transition to the ground state suggest the presence of a  $\nu(3s_{1/2}) \otimes [2_1^+ \otimes 3^-]_1$  component for the configuration of the 3227.9-keV level, where the  $2_1^+ \otimes 3^-$  coupling is due to mixing of the  $2_1^+$  and  $3^-$  states of  $^{88}\text{Sr}$ , and with a resulting  $J^\pi$  assignment of  $\frac{1}{2}^-$  or  $\frac{3}{2}^-$ . An admixture of the  $\nu(2d_{5/2}) \otimes 3^-$  component to the configuration could account for the weak ground-state transition as well as the  $\beta$  decay to the 3227.9-keV level through the same type of matrix elements that can account for  $\beta$  decay to the 2280.0-keV level. With this type of admixed configuration, the  $\gamma$ -ray transition between the 3227.9- and 2280.0-keV level would be collective  $E2$ , the transition to the 1031.88-keV level would be collective  $E1$ , and the ground-state transition would be particle-inhibited  $E1$  or  $E3$ .

The experimental results for the  $^{89}\text{Sr}$  ground state and the 1031.88-, 2280.0-, and 3227.9-keV levels and the suggested wave functions are summarized on Fig. 3. The configuration suggested for the 2280.0-keV level is based on the rather strong evidence of the collective transition to the 1031.88-keV level. That proposed for the 3227.9-keV level is consistent with the  $\gamma$ -ray and  $\beta$  tran-

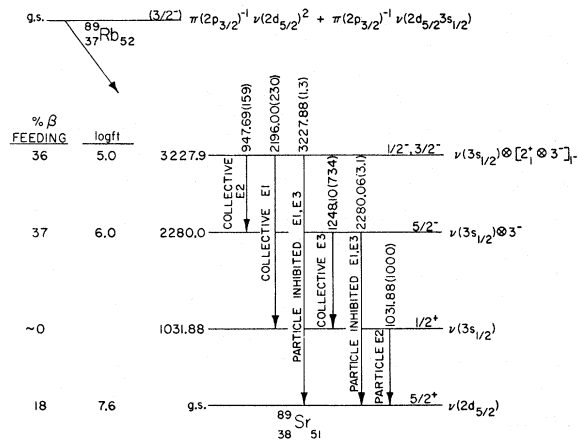


FIG. 3. A partial level scheme for  $^{89}\text{Sr}$  showing the properties of the 2280.0- and 3227.9-keV levels.

sition information, but the multiple coupling suggested should be regarded as speculative. Future studies should be devised to test this interesting character.

Experimental results indicate that the remaining levels below 3.5 MeV have positive parity and result from the  $2d_{3/2}$  and  $1g_{7/2}$  single-neutron states and from the single-neutron states coupled to the  $2_1^+$  state in  $^{88}\text{Sr}$ . Reaction studies<sup>8,10,13</sup> of the 2007.54-keV level show that it has a  $J^\pi$  of  $\frac{3}{2}^+$  and suggest a state configuration given by  $\psi = a\nu(2d_{3/2}) + \sum_j b_j \varphi_j \otimes 2_1^+$ , where  $a^2 = 0.46$ ,  $\sum_j b_j^2 = 0.54$ , and the  $\varphi_j$  are the neutron positive-parity states which can couple with the  $^{88}\text{Sr}$   $2_1^+$  level to give a  $J^\pi$  of  $\frac{3}{2}^+$ . This  $J^\pi$  assignment to the 2007.54-keV level is supported in this work by a  $\log ft$  value of 8.1 for the  $\beta$  branch to that level, and the numerous  $\gamma$ -ray transitions to the level from higher levels are indicative of a complex-state configuration.

The levels at 1473.22, 1940.23, 2058.0, and 2451.7 keV are candidates for the  $\nu(2d_{5/2}) \otimes 2_1^+$  coupled multiplet. The particle-core coupled nature of the 1473.22-keV level is supported by the nonstripping shape of the outgoing-proton distribution in  $(d, p)$  reactions.<sup>10</sup> The  $\log ft$  value of the  $\beta$  branch to this level is 8.7 using a statistical  $\beta$ -spectrum shape, and 9.1 assuming a unique  $\beta$ -spectrum shape. The magnitude of this  $\log ft$  value is consistent with a unique first-forbidden  $\beta$  transition ( $\Delta J = \pm 2$ , yes) and a  $J^\pi$  assignment of  $\frac{7}{2}^+$  to 1473.22-keV level. The  $J^\pi$  assignments of  $\frac{5}{2}^+$ ,  $\frac{3}{2}^+$  for the 1940.23-keV level,  $\frac{1}{2}^+$ ,  $\frac{3}{2}^+$ ,  $\frac{5}{2}^+$  for the 2058.0-keV level, and  $\frac{3}{2}^+$ ,  $\frac{5}{2}^+$  for the 2451.7-keV level are suggested by the  $\beta$ -transition  $\log ft$  values and a correspondence of these levels to levels found in  $(d, p)$  reactions.<sup>10</sup> The  $\frac{9}{2}^+$  level be-

longing to the  $\nu(2d_{5/2}) \otimes 2_1^+$  multiplet is not seen in this work, a result not unexpected because of spin and parity considerations. Hughes<sup>15</sup> calculates that this  $\frac{9}{2}^+$  level should be located at approximately 2080 keV. Assuming that  $\frac{9}{2}^+$  level is at 2080 keV and that the 1473.22-, 1940.23-, 2058.0-, and 2451.7-keV levels result entirely from the  $\nu(2d_{5/2}) \otimes 2^+$  configuration, the weighted average of the energies of this multiplet is 1935 keV, only about 100 keV more than the energy of the  $2_1^+$  level in  $^{88}\text{Sr}$ .

The  $\nu(3s_{1/2}) \otimes 2_1^+$  and (to a lesser degree)  $\nu(2d_{5/2}) \otimes 2_1^+$  couplings appear to be the major constituents of the 2570.14-keV-level wave function, since it is populated strongly from the 3227.9-keV level, and its most intense depopulating transitions are to the 2280.0- and 1031.88-keV levels and to the ground state. The resulting  $J^\pi$  assignment of  $\frac{3}{2}^+$ ,  $\frac{5}{2}^+$  is supported by the nonunique first-forbidden  $\beta$  transition indicated by a  $\beta$ -transition  $\log ft$  value of 6.8, while the collective nature of the level is supported by a nonstripping proton distribution in  $(d, p)$  reactions.<sup>10</sup> Assuming  $E2$  transitions with no substantial admixtures to the ground state and the first excited state, the 2570.14-keV level configuration, as calculated from the observed relative intensities of the 2570.14-, and 1538.08-keV  $\gamma$  rays, is  $\psi = (0.78)^{1/2} \nu(3s_{1/2}) \otimes 2_1^+ + (0.22)^{1/2} \nu(2d_{5/2}) \otimes 2_1^+$ .

Stripping reactions<sup>10</sup> and  $^{88}\text{Sr}(p, p)$  elastic scattering results<sup>13</sup> indicate that the  $1g_{7/2}$  neutron level is near 2700 keV in  $^{89}\text{Sr}$  and is largely single-particle in nature. The level at 2707.20 keV, with its intense ground-state transition and with no transition to the  $\nu(3s_{1/2})$  first excited level, probably corresponds to this  $1g_{7/2}$  single-neutron state with a resulting  $\frac{7}{2}^+$   $J^\pi$  assignment. However, the  $\log ft$  value of 6.8 for the  $\beta$  branch to this level is too small for the necessary unique first-forbidden  $\beta$  transition. This low  $\log ft$  value could be accounted for by minute  $\nu(2d_{5/2})(1g_{7/2})$  mixing in the  $^{89}\text{Rb}$  ground state.

The level at 3508.8 keV is given a  $J^\pi$  assignment of  $\frac{5}{2}^-$  on the basis of its  $\beta$ -transition  $\log ft$  value of 6.0, the strong transition to the ground state, and the absence of a transition to the first excited level [which thus rules out a  $\nu(3s_{1/2}) \otimes 3^-$  component for the 3508.8-keV level configuration]. The likely configuration for this level is a combination of single-particle states coupled to the  $3^-$  state of  $^{88}\text{Sr}$ , with the  $\nu(2d_{5/2}) \otimes 3^-$  component predominant.

In summarizing the  $^{89}\text{Sr}$  level scheme, it is seen that the properties of the ground state and the 1031.88-, 2007.54-, and 2707.20-keV levels are consistent with the  $2d_{5/2}$ ,  $3s_{1/2}$ ,  $2d_{3/2}$ , and  $1g_{7/2}$  neutron single-particle levels, respectively, though the  $2d_{3/2}$  strength is more diffuse than that



of the other single-particle states. The remaining positive-parity levels below 3 MeV can be accounted for by coupling the  $2d_{5/2}$  and  $3s_{1/2}$  neutron states to the  $2_1^+$  state of  $^{88}\text{Sr}$ . For the negative-parity levels at 2280.0, 3227.9 and 3508.8 keV, the transitions observed indicate strongly that the 2280.0-keV level configuration has a principal component of  $\nu(3s_{1/2}) \otimes 3^-$  and that for the 3508.8-keV level is mainly  $\nu(2d_{5/2}) \otimes 3^-$ . The level at 3227.9 keV appears to have a mixture of  $\nu(2d_{5/2}) \otimes 3^-$  and  $\nu(3s_{1/2}) \otimes [2_1^- \otimes 3^-]_1$ -configurations, the latter component, though surprising, being needed to explain the intense transitions depopulating this level to the 1031.88-keV and 2280.0-keV levels.

### B. $^{89}\text{Rb}$ Level Scheme

In a strict shell-model picture, the  $^{89}\text{Kr}$  ground state is probably described by three  $2d_{5/2}$  neutrons coupled to  $\frac{5}{2}^+$  with seniority 1, and with all protons paired. Thus,  $\beta$  decay to the  $\pi(2p_{3/2})^3(1f_{5/2})^6\nu(2d_{5/2})^2$   $^{89}\text{Rb}$  ground state would be first forbidden. The 14% ground-state  $\beta$  branch from  $^{89}\text{Kr}$  decay found in this work, in conjunction with a 4.93-MeV  $Q_\beta$  results in a  $\log ft$  value of 7.2, in good agreement with a first-forbidden  $\beta$  transition.

In discussing the excited levels of  $^{89}\text{Rb}$ , the only information available is the  $\beta$ -transition  $\log ft$  values and the  $\gamma$ -ray transitions between levels, since no reaction work has been reported on  $^{89}\text{Rb}$ . However, on the basis of shell-model states, the two lowest  $^{89}\text{Rb}$  excited levels at 220.90 and 497.5 keV probably have  $\pi(2p_{3/2})^4(1f_{5/2})^5\nu(2d_{5/2})^2$  and  $\pi(2p_{3/2})^2(1f_{5/2})^6(2p_{1/2})^1\nu(2d_{5/2})^2$  configurations, respectively,

with resulting  $\frac{5}{2}^-$  and  $\frac{1}{2}^- J^\pi$  assignments. These configurations are consistent with the  $\gamma$  and  $\beta$  transitions observed which involve these two levels and the  $^{89}\text{Kr}$  and  $^{89}\text{Rb}$  ground states. Tentative spin and parity assignments to the higher excited levels, indicated on the  $^{89}\text{Rb}$  level scheme, are based solely on (sometimes liberal) interpretation of the  $\log ft$  values and order-of-magnitude arguments about comparisons of relative intensities from reasonable assumptions for multipolarities of depopulating transitions. These  $J^\pi$  assignments should be regarded as tentative and subject to future affirmation; a supporting reaction study such as  $^{87}\text{Rb}(t, p)^{89}\text{Rb}$  would be most welcome and helpful.

In attempting to qualitatively account for the levels seen in  $^{89}\text{Rb}$ , one can appeal to a particle-core coupling model like that used in discussing the  $^{89}\text{Sr}$  level structure. The  $2p_{3/2}$ ,  $1f_{5/2}$ , and  $2p_{1/2}$  proton states are available to couple to the quadrupole-vibration states of neighboring even-even nuclei to account for many negative-parity levels, while the  $1g_{9/2}$  proton states and its coupling to quadrupole states could account for positive-parity levels. It may prove necessary, however, to assume a more complex model to account for the  $^{89}\text{Rb}$  level scheme, such as the Coriolis coupling model which has been applied to lower mass rubidium isotopes,<sup>25</sup> or to an anharmonic vibrator model.

The authors would like to express their appreciation to Dr. B. S. Cooper and Dr. S. A. Williams for fruitful discussions concerning the interpretation of the results of this work.

<sup>1</sup>G. H. Carlson, W. C. Schick, Jr., W. L. Talbert, Jr., and F. K. Wahn, Nucl. Phys. **A125**, 267 (1969).

<sup>2</sup>J. T. Larsen, W. L. Talbert, Jr., and J. R. McConnell, Phys. Rev. C **3**, 1372 (1971).

<sup>3</sup>W. C. Schick, Jr., W. L. Talbert, Jr., and J. R. McConnell, Phys. Rev. C **4**, 507 (1971).

<sup>4</sup>R. J. Olson, W. L. Talbert, Jr., and J. R. McConnell, Phys. Rev. C **5**, 2095 (1972).

<sup>5</sup>F. K. Wahn, W. L. Talbert, Jr., and J. K. Halbig, Nucl. Phys. **A152**, 561 (1970).

<sup>6</sup>W. L. Talbert, Jr. and J. R. McConnell, Arkiv Fysik **36**, 99 (1967).

<sup>7</sup>J. E. Kitching and M. W. Johns, Can. J. Phys. **44**, 2661 (1966).

<sup>8</sup>B. L. Cohen, Phys. Rev. **125**, 1358 (1962).

<sup>9</sup>R. L. Preston, M. B. Sampson, and H. J. Marten, Can. J. Phys. **42**, 321 (1964).

<sup>10</sup>E. R. Cosman, H. A. Enge, and A. Sperduto, Phys. Rev. **165**, 1175 (1968).

<sup>11</sup>E. R. Cosman, H. A. Enge, and A. Sperduto, Phys. Letters **22**, 195 (1966).

<sup>12</sup>E. R. Cosman, J. M. Joyce, and S. M. Shafroth, Nucl. Phys. **A108**, 519 (1968).

<sup>13</sup>E. R. Cosman, R. Kalish, D. D. Armstrong, and H. C. Britt, Phys. Rev. C **1**, 945 (1970).

<sup>14</sup>N. Auerbach, Phys. Letters **27B**, 127 (1968).

<sup>15</sup>T. A. Hughes, Phys. Rev. **181**, 1586 (1969).

<sup>16</sup>J. D. Vergados, Nucl. Phys. **A166**, 285 (1971).

<sup>17</sup>J. E. Kitching and M. W. Johns, Nucl. Phys. **A98**, 337 (1967).

<sup>18</sup>W. F. S. Poehlman, thesis, McMaster University, 1972 (unpublished).

<sup>19</sup>J. H. Norman, W. L. Talbert, Jr., and D. M. Roberts, U. S. Atomic Energy Commission Report No. 1S-1893, 1968 (unpublished).

<sup>20</sup>E. A. Henry, thesis, Iowa State University, 1972 (unpublished).

<sup>21</sup>J. R. Clifford, thesis, Iowa State University, 1972 (unpublished).

<sup>22</sup>C. M. Lederer, J. M. Hollander, and I. Perlman, *Table of Isotopes* (Wiley, New York, 1968), 6th ed.

<sup>23</sup>L. M. Langer and H. C. Price, Jr., Phys. Rev. **76**, 641 (1949).

<sup>24</sup>S. Shastri, Nucl. Phys. **A142**, 12 (1970).

<sup>25</sup>W. Scholz and F. B. Malik, Phys. Rev. **176**, 1355 (1968).